



Published in final edited form as:

*Reprod Toxicol.* 2015 August 15; 56: 32–44. doi:10.1016/j.reprotox.2015.06.047.

## Expression of tight junction proteins and transporters for xenobiotic metabolism at the blood-CSF barrier during development in the nonhuman primate (*P.hamadryas*)

C. Joakim Ek<sup>1,\*</sup>, Barbara D'Angelo<sup>1</sup>, Christine Lehner<sup>2</sup>, Peter Nathanielsz<sup>3</sup>, Cun Li<sup>3</sup>, and Carina Mallard<sup>1</sup>

<sup>1</sup>Institute for Neuroscience and Physiology, Department of Physiology, Sahlgrenska Academy, University of Gothenburg, 40530 Gothenburg, Sweden

<sup>2</sup>Institute of Tendon and Bone Regeneration, Paracelsus Medical University - Spinal Cord Injury and Tissue Regeneration Center Salzburg, Salzburg, Austria; Department of Traumatology and Sports Injuries, Paracelsus Medical University Salzburg, Austria; Austrian Cluster for Tissue Regeneration Vienna, Austria

<sup>3</sup>Wyoming Pregnancy and Life Course Health Center, University of Wyoming, Laramie Wyoming, United States 82071

### Abstract

The choroid plexus (CP) is rich in barrier mechanisms including transporters and enzymes which can influence drug disposition between blood and brain. We have limited knowledge of their state in fetus. We have studied barrier mechanisms along with metabolism and transporters influencing xenobiotics, using RNAseq and protein analysis, in the CP during the second-half of gestation in a nonhuman primate (*P.hamadryas*). There were no differences in the expression of the tight-junctions at the CP suggesting a well-formed fetal blood-CSF barrier during this period of gestation. Further, the fetal CP express many enzymes for phase I–III metabolisms as well as transporters suggesting that it can greatly influence drug disposition and has a significant machinery to deactivate reactive molecules with only minor gestational changes. In summary, the study suggests that from, at least, midgestation, the CP in the nonhuman primate is restrictive and express most known genes associated with barrier function and transport.

### Keywords

choroid plexus; fetus; primate; nonhuman; baboon; xenobiotic transport; neuroprotection; drug metabolism; blood-CSF barrier

---

\*Correspondence: Dr Joakim Ek, Inst. for Neuroscience and Physiology, University of Gothenburg, Medicinaregatan 11, Box 432, 40530 Göteborg, Sweden, Phone: +46 31 7863875, joakim.ek@neuro.gu.se.

**Publisher's Disclaimer:** This is a PDF file of an unedited manuscript that has been accepted for publication. As a service to our customers we are providing this early version of the manuscript. The manuscript will undergo copyediting, typesetting, and review of the resulting proof before it is published in its final citable form. Please note that during the production process errors may be discovered which could affect the content, and all legal disclaimers that apply to the journal pertain.

## 1. Introduction

The choroid plexus, which is situated in the ventricles of the brain, is the main blood-CSF interface. It contains a range of mechanisms to either prevent or facilitate transport of compounds across the choroid plexus epithelium. One important mechanism of the barrier is to protect the brain from potentially harmful exogenous or endogenous compounds. The plexus is well adapted for high transport of compounds from the blood to the cerebrospinal fluid. It contains a richly vascularised core with fenestrated vessels for promoting flux of fluid and compounds. Outside of the blood vessels is a continuous epithelium that is the main cellular barrier. These cells have highly complex tight-junctions insuring selective transfer by forcing flux of compounds across, rather than between, the epithelial cells that contain a battery of transporters and receptors. The tight-junctions have been shown to be restrictive already early in rodent development [1, 2]. Many of the transporters have roles in the production of the cerebrospinal fluid or are important for the influx of nutrients to the central nervous system as well as the homeostasis of the brain.

The epithelial cells contain a range of enzymes and metabolic activities that act as a defence for the central nervous system to reduce xenobiotic loading on the brain (Miller et al 2001; [3]. Metabolism in the plexus can also make lipid-soluble compounds more hydrophilic and increases the time that they are available for further metabolisms or exclusion by the plexus. Drug metabolising mechanisms have been shown to be present throughout the brain but are enriched at the blood-CNS interfaces, such as the blood-brain and blood-CSF barriers, where they can act as an outer defence against access to the brain [4]. Several drug metabolising mechanisms are present in the developing plexus, including the energy-driven ATP-binding cassette proteins such as breast cancer related protein (BCRP) and multi-drug resistance related proteins in the ABC family [5, 6]. Transport by these pumps may be facilitated by phase II metabolism of compounds including conjugation of glutathione, sulfation and glucuronidation. A wide variety of other solute carriers are also present on choroidal epithelial cells belonging to the SLC- or SLCO-families that are indicated in drug transport. Previous studies have demonstrated that at least some of these mechanisms are working at a similar level in the fetus as in the adult [7]. A WHO sponsored investigation showed that women ingest an average of three prescription medications during pregnancy [8]. There is also a growing concern how environmental toxins affects the development of the brain [9]. An important question in regard to the potential harmful effects on the fetal brain in relation to xenobiotics such as drugs in the maternal circulation is therefore how well the defence mechanisms at the blood-CNS interfaces are developed in the fetus. Recently the gene changes of drug metabolising and antioxidant systems were reported for the developing rat choroid plexus [10]. In order to further our understanding of these defence mechanisms at the choroid plexus in a translational model we sourced choroid plexus from a fetal nonhuman primate, the baboon (*P. hamadryas*), which has very close development to the human. Our study was conducted during the second half of gestation when the majority of the cortical expansion is occurring in primates [11]. We firstly investigated the genes and proteins associated with cell-junctions at the blood-CSF barrier and secondly explored changes in genes related to drug transport, metabolism, antioxidant defence and CSF production.

## 2. Material and Methods

### 2.1 Animals

Female baboons (*Papio hamadryas*) from the Southwest National Primate Research Center (San Antonio, TX, USA) were used for this study. All procedures were approved by the Institutional Animal Care and Use Committee of the Texas Biomedical Research Institute and conducted in AAALAC-approved facilities. Feeding and management have previously been explained in detail [12]. Food was withdrawn for 16 hours before surgery. Caesarean sections were performed at 90 (50% gestation), 120 (67% gestation) and 165 days (90% gestation) of gestation (term 184 days) under general anaesthesia as previously reported [13]. Following caesarean section maternal analgesia was provided with buprenorphine hydrochloride 0.015 mg/kg per day (Hospital, Inc., Lake Forest, IL, USA) for three days post-surgery. When caesarean section was performed to obtain samples from multiple areas of the brain and other fetal tissues, fetal telencephalic choroid plexus (lateral ventricular plexus) was collected and frozen in liquid nitrogen at gestation day (GD) 90 (2 males/1 female), GD120 (2 males/2 females) and GD165 (3 males/3 females). Choroid plexus was also obtained from two non-pregnant adult females at 9.4 and 10.2 years of age and two pregnant baboons at 9.4 and 11.3 years of age. These adult animals were necropsied as part of a wider study of aging. Where euthanasia was performed on foetuses and adult animals it was conducted by exsanguination while the animal was under general anesthesia as approved by the American Veterinary Medical Association.

### 2.2 RNA Preparation and RNA sequencing

A detailed description of RNA sequencing has been published elsewhere [14]. Briefly, frozen tissues were homogenised and RNA extracted with an RNeasy mini-kit (Qiagen) according to manufacturer's specifications. RNA quality was analysed by Biorad Experion electrophoresis. RNA-seq was performed at the Genomics Core Facility at University of Gothenburg. Only high quality RNA was used for library preparation (RIN >8). Libraries were created using the TruSeq™ RNA Sample Preparation v2 kit and the library was subjected to 50bp single end read cycles of sequencing on an Illumina HiScan SQ.

### 2.3 Analysis of sequencing data

RNA-seq reads were mapped to the current baboon genome assembly (<https://www.hgsc.bcm.edu/content/baboon-genome-project>) using Tophat [15]. Cufflinks [16] was used for transcript assembly of individual samples. All assemblies were merged to create a reference transcript, which was used to calculate gene counts with HTSeq (<http://www-huber.embl.de/users/anders/HTSeq/doc/overview.html>). DESeq [17] was then used to find differentially expressed genes. Annotation of genes was done through blasting (blastx) (Altschul et al., 1990) each transcript against the Swiss-Prot database (Uniprot Consortium). Differential expression of transcripts was considered between GD90 and GD165 with *p*-value considered significant when less than 0.05. The expression levels for genes were divided into five levels for the Results section whereby normalised raw counts between 1–10 were considered very low expression, 10–100 low expression, 100–1000 medium expression and 1000–10000 high expression and >10000 very high expression. The cut-off detection level was set to 1 (i.e. all transcripts where the raw read count was less than 1 across all ages

were removed). In addition, we have not further deliberated on significant changes in genes for which expression was limited to the very low expression range (<10 counts) across all developmental ages. Changes in genes were visualised in heatmaps generated in the statistical software R along with cluster analysis. We have used GO terms for human proteins annotated to tight-junction and cell-cell adhesion to make relevant heatmaps of genes associated to these terms, however, genes were also manually collated with duplicates removed.

## 2.4 Immunohistochemistry (IHC)

After fixation for 24 hours in 4% paraformaldehyde, plexuses from fetuses at GD120, GD165 and adults (no GD90 animals were available) were dehydrated in increasing concentrations of alcohol and embedded in paraffin. Serial sections were cut on a microtome and prepared for IHC. Paraffin was removed from sections in xylene, sections were rehydrated in decreasing concentrations of ethanol and gently boiled in 0.01 M citrate buffer or protease digestion (*Streptomyces griseus*, Sigma; 1 mg/ml at 37°C) for 10 min. Blocking steps included H<sub>2</sub>O<sub>2</sub> treatment (3% in methanol for 10min) and appropriate serum (5%) or DAKO serum-free protein block for 1 hour. Sections were then incubated in the following primary antibodies towards three key plexus tight-junctional proteins: ZO-1 (1:100; Cat#61-7300, Invitrogen), occludin (1:100; Cat#71-1500, Invitrogen) and claudin-1 (1:200; Cat#71-1500, Invitrogen). They were then incubated in biotinylated secondary against the appropriate species followed by the ABC kit (Vector) or HRP-labelled secondary antibody (BrightVision poly HRP-anti-rabbit IgG from ImmunoLogic) and developed with DAB. In between all steps, sections were washed in PBS with 0.1% tween20. After 5 minute in DAB solution, sections were washed in water, dehydrated and cover-slipped. Blank sections were obtained when primary antibody was omitted.

## 2.5 Protein analysis

Choroid plexus tissues (from the same samples as for RNAseq) were homogenised by sonication in ice-cold PBS containing 5mM EDTA, protease inhibitor cocktail (PIC, P8340, Sigma), phosphatase inhibitor cocktail 1 (P2850, Sigma), phosphatase inhibitor cocktail 2 (P5726, Sigma). The protein concentration was determined using a spectrophotometer at 280-nm absorbance. Sample lysates were mixed with 5X Laemmli sample buffer and heated (70 C) for 10 min. To detect occludin and claudin-1 proteins 10 µg of total protein extract was resolve on 4–12% Tris–glycine gels (Novex, San Diego, CA, USA); For ZO-1 20µg of total protein was resolve on 3–8% Tris–acetate gel (Novex, San Diego, CA, USA). After electrophoresis, proteins were transferred to reinforced nitrocellulose membranes (Schleicher & Schuell, Dassel, Germany) and membranes blocked in 30 mM Tris–HCl (pH 7.5), 100 mM NaCl and 0.1% Tween-20 (TBS-T) containing 5% fat-free milk powder for 1 h at room temperature. Then, the membranes were incubated overnight at 4 °C with the following primary antibodies in 5% bovine serum albumin (BSA)-TBST: rabbit anti-occludin, 1:2000, rabbit-anti claudin-1, 1:1000, rabbit anti-ZO-1, 1:400 (Invitrogen, CA, USA) and rabbit anti-β-actin, 1:10000 (Sigma-Aldrich, St. Louis, MO, USA) or mouse anti-GADPH, 1:500 (Abcam, Cambridge Science Park, Cambridge, UK). After washing, the membranes were incubated with peroxidase-labelled goat anti-rabbit or anti mouse (1: 5000) secondary antibody (Vector Laboratories, Burlingame, CA, USA) at room temperature.

Immunoreactive species were visualised using the Super Signal Western Dura substrate (Pierce, Rockford, IL, USA) and a LAS 1000-cooled CCD camera (Fujifilm, Tokyo, Japan). Immunoreactive bands were quantified using the Image Gauge software (Fujifilm) and normalised with respect to  $\beta$ -actin or GAPDH. Data were analysed across ages with one-way ANOVA using SPSS software ( $\alpha < 0.05$ ).

### 3. RESULTS

#### 3.1 Tight-junctional proteins

##### 3.1.1 Western blotting and immunolocalisation of tight-junctional proteins—

We used immunohistochemistry to investigate the localisation of occludin, ZO-1 and claudin-1 proteins in the fetus and adult. All three proteins showed almost identical immunolocalisation at the apical cell membrane of epithelial cells (Figure 1). There was no difference in the staining pattern between the fetal ages or adults. We also used western blotting to quantitatively investigate the expression level of the three tight-junctional proteins in the fetal plexus (Figure 2). Western blotting produced bands in blots at expected sizes for each tight junctional protein (occludin ~ 60KDa, claudin-1 ~ 20KDa and ZO-1 ~ 225KDa) although an additional band at around 70KDa was detected for ZO-1. Protein quantification using western blotting showed that all three proteins were present in the choroid plexus in the 90, 120 and 165 GD plexus. There were only minor changes in protein levels of all three proteins during fetal development and it was only ZO-1 that showed a somewhat higher level at the intermediate age (GD120) but this did not reach statistical significance ( $p=0.13$ ).

##### 3.1.2 Tight-junction and cell-adhesion associated genes—

To further investigate cell-junction mechanisms at the fetal blood-CSF barrier we collated all genes associated to tight-junction and cell-adhesion across the three gestational ages (Figure 3). For tight-junction associated genes (Figure 3A) the GD90 animals showed the highest transcription of these genes with few changes in the genes between GD120 and GD165. This was also signified in the cluster analysis, which showed that GD90 animals form a separate group whereas GD120 and GD165 animals form a mixed group. A more distinct pattern is seen for cell-adhesion genes (Figure 3B). In this group of genes there was a stepwise reduction of transcription during gestation with GD90 having the highest transcription and GD165 the lowest. The cluster analysis for cell-adhesion genes showed that all animals cluster consistently within their respective gestational age group.

#### 3.2 Xenobiotic Metabolism and Transport

Xenobiotic metabolism is commonly divided into three phases whereby in phase I polar groups are added to compounds and in phase II, charged species are added to compounds such as glutathione, sulphate or glucuronic acid. Phase I/II metabolism makes compounds less lipid soluble and less likely to cross into the brain. In phase III metabolisms compounds are excreted by transport proteins such as the ATP-binding cassette proteins (ABC-proteins). We divided changes in genes in these three stages of metabolism and further explored other solute carriers that are important for xenobiotic transport as well as oxidative stress. Age-

dependent regulation of proteins refers to significant expression differences between GD90 and GD165. Results are presented in Tables 1–5.

**3.2.1 Xenobiotic Metabolisms - Phase I**—In total 25 different iso-enzymes of cytochrome P-450 monooxygenases (CYPs) were detected (Table 1; Suppl. Fig. 1). The highest number of transcripts was found in the CYP2 (*CYP2A6/C8/C18/C19/J2/R1/S1/W1*) and CYP4 (*B1/F11/F12/V2/X1/Z1*) families representing 56% of all CYPs detected. Only *CYP1B1* and *CYP3A5* were detected within their respective family. Most were in the very low or low expression level with five in the medium level (*CYP1B1*, *CYP2R1/W1*, *CYP4F12/V2*). Three CYPs showed regulation during fetal development with *CYP2S1* increasing 3.02 fold, *CYP2W1* decreasing 25.4 times and *CYP4F12* increasing 4.64 fold from GD90 to GD165. Transcripts for the epoxide hydrolases *EPHX1/2* were transcribed in the high range, *EPHX3* in medium range and *EPHX4* in the low range. Up-regulation during development occurred in both *EPHX1/2* with 1.81 and 1.60 fold higher expression at GD165 compared to GD90, whereas *EPHX4* was down-regulated 2.06 times during gestation. Transcription for monoamine oxidase *MAO1* was in the medium range and *MAO2* in the high range. *MAO1* was significantly down-regulated from GD90 to GD165 (–2.49 times) whereas *MAO2* was significantly upregulated (1.53 times).

**3.2.2 Xenobiotic Metabolism - Phase II**—We detected in total fourteen Glutathione S-transferases (GSTs) belonging to the  $\alpha$  (*GSTA1/3/4*), (*GSTM1/2/3/4/5*),  $\kappa$  (*GSTK1*),  $\omega$  (*GSTO1*), (*GSTP1*),  $\zeta$  (*GSTZ1*) and  $\theta$  (*GSTT1/2*) classes with the only class not detectable being  $\sigma$  (Table 2; Suppl. Fig 2). Nearly all GST transcripts were in the medium or high range of expression with highest expression levels found for *GSTM3*, *GSTM5*, *GSTK1* and *GSTP1*. Five microsomal GSTs (*MGST1-3*, *LTC4S*, *PTGES*) were also detected. *MGST1-3* and *LTC4S* were transcribed at the medium range with no developmental regulation whereas *PTGES* expressed at low level. The only regulated soluble GSTs were *GSTK1* which was increased 2.49 during gestation whereas the only regulated microsomal GSTs was *PTGES*, which was down-regulated 1.86 times. Cytosolic glutathione reductase (*GSR*), maintaining glutathione in the reduced form, showed high expression levels across all ages and was significantly upregulated 1.96 times during gestation. *GCLM* (glutamate-cysteine ligase regulatory subunit) and *GCLC* (glutamate-cysteine ligase catalytic subunit), the first rate limiting enzymes in glutathione production, showed high and medium expression levels with no fetal regulation. Glutathione synthetase (*GSS*), which catalyses the last step of glutathione production showed medium expression with no developmental regulation.

Five sulfotransferases (SULTs) were detected in the choroid plexus (*SULT1A1/A3/C4/E1*, *SULT4E1*), with the highest expression being *SULT1A3* with no developmental regulation. The only age-regulated SULT gene was *SULT1E1*, which was down-regulated 11.6 fold from GD90 to GD165. Only one UDP-Glucuronosyltransferase, *UGT3A1*, was detected in the very low level of expression at GD90/120 but was under the detection range at GD165.

Some other transferases are also considered important for phase II metabolism of xenobiotics [18]. Expression of the arylamine N- acetyltransferases *NAT1/2* were detected, but both transcribed at a very low level. We could not detect both thiopurine S-

methyltransferase (*TSMT*) and catechol O-methyltransferase (*COMT*) at a high expression level in the choroid plexus with no developmental regulation.

**3.2.3. Xenobiotic Metabolisms - Phase III**—It is mainly the ABCB- and ABCC-families as well as ABCG2 that are important for xenobiotic transport. Within the ABCC family, encoding for the multi-drug resistance related proteins (MRPs), we detected nine variants (*ABCC1-6*, *ABCC8-10*), all in very low to medium expression level with *ABCC1/C4* having the highest expression across all ages (Table 3; Suppl. Fig. 3). *ABCC1/MRP1* and *ABCC4/MRP4* were the only regulated transcripts with *ABCC1* down-regulated 2.37 times whereas *ABCC4* was upregulated 2.44 times from GD90 to GD165. We could also specifically identify isoform 6 and 8 of *ABCC1* protein, which both showed significant down-regulation with age (−3.26 and −4.88 fold, respectively). Within the ABCB family 6 forms were detected (*ABCB1*, *ABCB6-10*) with *ABCB1/B8* in the medium range and *ABCB6* in the high range. *ABCB1/MDR1* was down-regulated 2.22 times during gestation with no other ABCB genes regulated. ABCG2/BCRP decreased 1.91 times from GD90 to GD165 but the change was not significant (p=0.09).

**3.2.4. SLC transporters**—Within the solute carriers it is mainly the SLCO, SLC22, SLC47 and SLC15 families that are considered important in relation to pharmacological toxicology (Nigam 2015). We could detect transcription of eight genes in the SLCO family (formerly known as SLC21 family) with two in the very low (*SLCO1B7*, *SLCO4A1*), one in the low (*SLCO1B1*), three in medium (*SLCO1C1*, *SLCO2A1*, *SLCO2B1*) and three (*SLCO1A2*, *SLCO1B3*, *SLCO3A1*) in the high range (Table 4; Suppl. Fig 4). All but one (*SLCO4A1*) had significantly higher transcription at GD165 than at GD90 (1.49–27.5 times higher). Ten members of the SLC22A family were detected in the choroid plexus. Seven were in the very low or low range (*SLC22A2/A3/A15/A16/A18*), three in the medium range (*SLC22A6/A20/A23*) and two in the high range (*SLC22A5/A8*). *SLC22A8* was regulated during development with 2.31 fold higher expression at GD165 than at GD90 as well as *SLC22A23*, which was down-regulated 1.58 times during gestation. Within the SLC15 class of solute carriers we detected *SLC15A2/A3/A4* expression. *SLC15A4* showed expression in the high range, *SLC15A3* in the medium range and *SLC15A2* in the low range. Only *SLC15A2* showed age-dependent regulation whereby expression was significantly lower at GD165 than at GD90 (−2.34 times). We could detect medium expression of *SLC47A1* and high expression of *SLC47A2* in choroid plexus across all gestational ages. Both genes were upregulated from GD90 to GD165 with *SLC47A1* increasing 4.47 times and *SLC47A2* 7.62 times.

### 3.3 Antioxidant systems

Superoxide dismutase (SOD) 1 (soluble form), SOD2 (mitochondrial form) and SOD3 (extracellular form) were all detected in the choroid plexus (Table 5; Suppl. Fig 5). SOD1 showed high expression, SOD2 medium expression and SOD3 medium expression at GD90/GD120 but high at GD165. Both SOD1 and SOD3 were significantly increased at GD165 compared to GD90 increasing 2.39 and 21.9 times, respectively. The copper chaperone *CSS* gene, important for copper delivery to SOD1, was transcribed at medium levels across all ages with no developmental regulation. Both heme oxygenase-1 (*HMOX1*) and *HMOX2*

were detected in the medium range, but with *HMOX2* about 3 times higher than *HMOX1*. None were regulated with development of the choroid plexus.

Two factors are thought to have particular importance in turning on antioxidant response elements (ARE): peroxisome proliferator-activated receptor gamma coactivator-1 alpha (PGC1 $\alpha$ ) and nuclear factor-erythroid 2 (NF-E2) related factor 2 (NRF2). *PGC1A* was expressed at medium levels at GD90 but high levels at GD165 and this increase (+1.75 times) was significant. *PGC1B* was expressed at a very low level. The transcript of *NFE2L2* (encoding for NRF2) was expressed at high levels at all ages studied with no developmental regulation. Also the NRF2 regulating factor Kelch-like ECH-associated protein 1 (*KEAP1*) was expressed at high levels at all ages with no developmental regulation. Likewise, we found high expression of NRF1 gene (*NF2L1*) with no development regulation.

### 3.4 CSF production

The molecular mechanisms for the production of CSF are still not completely understood but are thought to rely on a range of membrane transporters, water channels, ion channels and enzymes. We have presented transcripts related to CSF production as based on Brown et al [19] and Janssen et al [20] giving a list of 41 transcripts in total that were detectable in the baboon choroid plexus (Table 6; Suppl. Fig 6). We found medium expression level for five of these (*AT1B1*, *CA4*, *SLC4A8*, *CLCN3*, *KCNF1*), high expression for eleven of these (*AT1A2*, *AT1B1-3*, *CA2/14*, *SLC4A5*, *SLC12A2/A7*, *CLCN7*, *KCNH2*) and very high for two transcripts (*AQP1* and *CA2*). Transcripts that were up-regulated between GD90 and GD165 were *AQP1* (1.91 times), *AT1A2* (3.63), *AT1B1* (4.11), *AT1B2* (1.83), *CA13* (2.61), *SLC4A8* (2.57), *SLC12A2* (1.40), *KCNH2* (1.94), *KCNK1* (2.63) and down-regulated were *CA9* (-1.94), *CLCN3* (-2.74), *KCNA4* (-4.65), *SCN5A* (-4.88).

## 4. DISCUSSION

We have investigated the blood-CSF barrier during the second half of nonhuman primate gestation using protein analysis for tight-junctional proteins and whole genome profiling, exploring enzymes and transporters with importance for xenobiotic metabolism and transfer as well as CSF production. Overall the data strongly indicate a well-developed choroid plexus barrier, with respect to tight junctions and development of many enzyme and xenobiotic transport mechanisms by mid-gestation. However, we did detect some genes associated with antioxidant systems being lower at midgestation compared to near-term.

### 4.1 Tight junction proteins

Firstly, we were interested in the age-dependent state of cell-junctions that make up the physical barrier at the choroid plexus. We focused on three key tight-junctional proteins; the transmembrane proteins occludin and claudin-1 as well as the tight-junctional anchoring protein ZO-1. These proteins were expressed in the apical cell membrane of epithelial cells as expected based on previous ultrastructure studies of choroidal epithelial cells [1] and mouse and human choroid plexus epithelium [21, 22]. We then examined the protein level of the tight junctions during gestation and showed similar expression across all ages. In order to further analyse molecular changes of cell-junction we explored gene transcription of tight-



junction and cell-adhesion associated genes. This analysis showed that the highest level of transcription for both these groups of genes occurred at the earliest gestational age studied (GD90). Taken together, these data substantiates the overall notion that the molecular basis for cell-junctions at the blood-CSF is well established at mid-gestation in the nonhuman primate although this needs to be tested and confirmed with functional studies. Additionally, the high expression of many solute carriers and ion transporters support a functioning diffusion barrier at the plexus. The data corroborate with previous functional studies in rats and marsupials which have shown that these tight-junctions are restrictive to even small molecules soon after choroid plexus differentiation [1, 2, 23] and with presence of tight-junctions proteins at the apical membrane in the fetal human plexus [22]. Restrictive cell junctions is of fundamental importance to the choroid plexus in order to operate as a barrier forming tissue since it insures flux of compounds through the epithelial cells (not between cells) and is a prerequisite for selective transfer of compounds in/out of CSF. In addition, this makes it achievable to maintain concentration gradients between blood and CSF. Such concentration gradients between CSF and blood have been shown to be established already by gestational day 50 (earliest age studied) in the rhesus monkey [24] and the authors conclude that this shows the presence of effective passive permeability barriers between blood and CSF in the fetus supporting our results.

## 4.2 Xenobiotic metabolism

As compounds pass through the cells in the choroid plexus they can be subjected to facilitated influx/efflux by transporters as well as exposed to metabolism. In addition, the choroid plexus is thought to maintain homeostasis in the brain by removing substances from CSF. We thus further explored changes in genes related to xenobiotic metabolism, efflux proteins, solute carriers as well as oxidative stress at the blood-CSF barrier.

**4.2.1 Phase I: xenobiotic metabolism**—The most important group of compounds for phase I metabolism is the CYP superfamily. We detected in total 25 different CYP transcripts, which amounts to around one third of all known human CYP monooxygenase genes. In contrast, only a small number of CYPs were found in the rat choroid plexus [10]. It is uncertain if the variance in numbers is due to different analysis platforms between studies or if it is a species difference between primates and rodents. We have data from neonatal mouse choroid plexus using the same Illumina platform as used in this study showing a similar number of CYPs in the baboon as in the mouse plexus (A. Motaheddin, unpublished). Although many CYPs were detected in the present study, most were expressed at low levels and their biological significance during development remains unclear. Similar to reports on the rat choroid plexus [10] we found much higher expression levels for the epoxide hydrolases and MAOs than CYPs. Overall there was also little regulation during gestation among the CYP genes (4/25 regulated). On the other hand 3/4 epoxy hydrolases were regulated, including the most abundant phase I transcripts, *MOA-B* and *EPX1/2*. The role of monoamine oxidases in xenobiotic metabolisms is not well studied however and our present data suggest that they may play a more important role for phase I metabolisms in the developing plexus than the CYPs.

**4.2.2 Phase II: xenobiotic metabolism**—Transferases play a central role in detoxification processes tagging xenobiotics or waste products for elimination. The transferases glutathione-s-transferases (GSTs), sulfotransferases (SULTs) and UDP-glucuronosyltransferases (UGTs) are important enzymes for phase II metabolism [18]. The primate choroid plexus was rich in GSTs with a total of fourteen transcripts detected. It is thought that it is mainly the  $\alpha$ ,  $\mu$  and  $\pi$  GST classes that are involved in drug metabolism [25]. Ten out of the 14 detected GSTs belong to these three classes suggesting a prominent role for GSTs in xenobiotic metabolism in the non-human primate choroid plexus during gestation. In addition, we found five microsomal GSTs. Microsomal GSTs are membrane bound and localised to the mitochondria and endoplasmic reticulum and are thought to protect these organelles from oxidative stress [25]. However, the exact role of the microsomal GSTs in relation to xenobiotic metabolisms is unclear at the moment and it has been difficult to study their specific contribution since they are masked by the activity of cytosolic GSTs.

Five SULTs were detected in the choroid plexus including *SULT1A1*, which has previously been shown to be transcribed and active in the rat choroid plexus [26]. The only regulated SULT-associated gene during gestation was *SULT1E1* (−10.8 times), which catalyses the sulphonation of estradiol and estrone so may play an important role for estrogen uptake into the brain during development. There was a striking lack of transcripts for UGTs suggesting a minor role for these in phase II metabolism at the blood-CSF barrier. In support, studies indicate that glucuronidation by UGTs mainly occurs in the liver [27].

From our data there is little to suggest that phase II metabolism enzymes changes during the second half of fetal development. Instead there is a considerable phase II metabolic capacity in the fetal choroid plexus mainly within the GST family. The data also suggest that the plexus is well equipped for production of glutathione. This is in agreement with previous studies showing high GST activity in the developing rat and human choroid plexus [7].

**4.2.3 Phase III: xenobiotic metabolism**—ABC-transporters can significantly alter drug distribution across cellular membranes such as the gut epithelium. Their prominent role in reducing entry of various drugs at the blood-CNS interfaces, including anti-cancer medication, antibiotics and immunosuppressants as well as environmental toxins, is well documented [28–30]. Although these transporters largely appear to work in conjugation with phase II metabolism some have also been shown to be able to directly efflux drugs that have not undergone previous metabolism [29]. In the present study we found a broad complement of ABC-transporters being transcribed at the blood-CSF barrier across all ages with very small changes during gestation. Since ABC-transporters are membrane bound their cellular localisation becomes important for the interpretation. MRP1 has been shown to specifically localise to the basolateral membrane of choroidal epithelial cells [5, 6] suggesting it does contribute to keeping xenobiotics out of the brain. Studies by Wijnold and colleagues have also suggested that MRP1/ABCC1 presence at the choroid plexus can significantly reduce drug disposition into the brain [31]. It is enriched at the blood-CSF barrier compared to the blood-brain barrier [6] and protein expression localise in the choroid plexus, but not in the blood-brain barrier [5, 6]. The down-regulation we detected in *ABCC1* is in contrast to rats where an increase has been shown during development in the plexus [5, 10], however, agrees

with data from mice [32]. ABCC4/MRP4 has also been shown to localise to basolateral membrane of choroidal epithelial cells and limits drug movement of topotecan from blood to CSF [33]. Cellular protein localisation of the many MRPs is uncertain across epithelia and endothelia due to the difficulty in reliable antibodies. In the ABCB family we could detect *ABCB1* and *ABCB6-10* with *ABCB6* the only transcript that showed high expression. To our knowledge there is no previous reports on MRP6/ABCC6 importance for drug disposition at the blood-brain barriers but it is suspected to confer anticancer drug resistance in cell lines and in particular protect against arsenic cytotoxicity [34]. The best known transporter related to drug efflux in this family is ABCB1 also known as p-glycoprotein. P-gp/ABCB1 can efflux drugs directly when passing through the cell membrane. P-gp deficient mice have dramatically increased brain tissue distribution and toxicity to several drugs such as cyclosporin A, etoposide, digoxin and dexamethasone [35] but the present data and previous studies suggest minor role at the blood-CSF barrier. *ABCB1* was expressed in the medium range and was significantly down-regulated from GD90 to GD165 (2.32 times), in agreement with studies of the rat choroid plexus with development [10] although it has been shown not to change in mice (Liddelow et al. 2012).

**4.2.4 Solute carriers**—The SLCO family (Solute Carrier Organic Anion), also known as organic anion transporting polypeptides (OATPs), is present on various epithelia across the body mediating primarily transport of large hydrophobic organic anions. Drug pharmacokinetics that are influenced by these transporters include B-blockers, statins and artans but numerous other drugs have been implemented in their transport and a very comprehensive list is given by [36]. This group of transporters showed the most consistent change during gestation with 7/8 transporters increasing during gestation with *SLCO1C1* the most regulated transporter in this family (+27.5 times). *Slco1c1* is also highly increased during development in the rat [10]. The SLCO1C1/OATP-F transporter has particular high affinity for hormones thyroxine and estrogen [37] but several of the other SLCO transporters also have affinity for these hormones [36]. The lower expression of these transporters at earlier gestation substantiates the question raised by [10] how sufficient levels of these hormones, which are important for early brain development, reach the brain. There is a particular high divergence of genes encoding for these transporters between human and rodents making comparisons and translation of functional studies difficult. For instance, *SLCO1A2* in humans encoding for OATP1A2 has five orthologues in the rat, *slco1a1* and *slco1a3-6*. Within the SLC22 family we found high expression of *SLC22A5/A8* similar to the rat choroid plexus. [38] found immunolocalisation of SLC22A6/OAT1 and SLC22A8/OAT3 to the human choroid plexus but membrane localisation was uncertain. In rats it has been shown that SLC22A6/OAT1 is present on the apical membrane is believed to remove substances from the CSF [39]. To our knowledge the membrane localisation of SLC22A5/OCTN2 or SLC22A8/OAT3 is not known in either rodents or human but would be of interest to know. There is considerable overlap of substrate specificity for these transporters making it difficult to study and interpret complement and changes at the choroid plexus. However, in general solute carriers facilitate the entry of compounds into the plexus in contrast to ABC transporters which limit their entry. The high expression of many SLCs in the plexus suggest that it contributes to the supply of nutrients to the developing brain and

that within the outlined SLC families there are minor changes in gestation regarding transport capacity.

We found a similar complement of SLC15 family of genes in the nonhuman primate as that previously reported in the rat choroid plexus [10]. In this family SLC15A2/PEPT2 has been shown to be important in relation to drug transport and has affinity for peptide-mimetic drugs (such as aclovir) and is present on the apical membrane on epithelial cells in the choroid plexus. Studies using choroid plexus epithelial cultures and PEPT2 knockout mice have suggested it removes peptides from the CSF [40, 41]. Specificity of PEPT3 and PEPT4 (encoded by SLC15A3/A4) does not seem to be known yet. Of note is also that we found transcription for SLC47A1/MATE1 and SLC47A2/MATE2 proteins in the choroid plexus which both increased during gestation, however, their function at this interface remains elusive.

**4.2.5 Antioxidants**—As has been suggested before [10] that antioxidant systems are likely to be important for choroid plexus epithelial cells since they are readily exposed to blood solutes through the rich vasculature of the plexus. In addition, the majority of reactive oxygen species are produced in mitochondria as a by-product of oxidative phosphorylation and the choroidal epithelial cells are abundant in mitochondria [1]. Although there was an increased level of expression of SOD genes at the latest fetal age, the data also shows that transcription is already high at mid-gestation. Antioxidant response elements (ARE) can be turned on in the event of oxidative stress and there are two factors that have emerged as master controllers for these responses [42]. PGC1 $\alpha$  is a regulator of mitochondrial biogenesis genes that simultaneously upregulates many genes known to protect against oxidative stress and NRF2, which turns on a battery of antioxidant genes but also xenobiotic metabolising enzymes. Together, PGC1 $\alpha$  and NRF2 activation drives glutathione synthesis, heme-oxygenases, SOD production and are thus important for antioxidant activity as well as drug metabolising with downstream effects on ABC-proteins. Most of the genes related to these two systems were transcribed at high levels across all gestational ages and there was little developmental regulation. Overall, this suggests that the fetal choroid plexus encompass significant antioxidant activity mechanisms. We have previously shown that the NRF2 system is turned on in the choroid plexus in neonatal mice in response to hypoxia-ischemia [43].

**4.2.6 CSF production**—A main site for the production of CSF is thought to be the choroid plexus although extra choroidal sources are probably also present and the classical view of CSF circulation has repeatedly been challenged [44]. The continual production and reabsorption of CSF act like a dilution process, traditionally known as the CSF sink effect, for substances entering the CNS and is therefore an governing factor determining CSF and brain concentrations. A relevant question in relation to neuroprotection of the fetus is therefore whether there are changes in the CSF production by the choroid plexus during fetal development. The molecular mechanisms behind CSF production is still tentative but is thought to be driven by the flux of Na, K, Cl and HCO $_3^-$  across the plexus epithelial cells with water movement regulated by aquaporins [19]. We have listed in Table 6 the level of transcripts thought to be related to CSF production [19, 20]. Although most of these

transcripts did not show regulation during gestation, of the twelve transcripts showing high or very high expression levels, half were up-regulated between GD90 and GD165 (*AQP1*, *AT1A2*, *AT1B1/2*, *SLC12A2*, *KCNH2*) with none down-regulated. If we believe that these twelve genes are the ones most pertinent for CSF production, then the data suggest that the CSF production is higher near-term for the nonhuman primate plexus cells. Of special note is the increase of both Na-K-Cl co-transporter *SLC12A2* and *AQP1*. *SLC12A2*, situated on the CSF-facing membrane of the epithelial cells is thought a key transporter for the production of CSF at the plexus [45]. *AQP1*, situated also on the apical membrane on epithelial cells, has previously been suggested as an important contributor of water movement across the plexus during CSF secretion [46, 47], which is supported by *AQP1* showing the highest expression of all genes outlined in our study. However, it is important to mention that to fully understand the effects of CSF production by plexus cells there is a need to take into account many other factors such as the growth of the plexus and changes in the ventricular system dynamics during development.

#### 4.3. Limitations of the study

One limitation of this study is that we have not compared gene transcription changes in the fetus with adult animals. To better understand the stage of fetal development such a comparison would be of interest and should be included in future work. It is also important to note that our anatomical and molecular analyses of the localisation and levels of tight-junctional genes and proteins are only indicative of barrier function and functional tests of the blood-CSF barrier should be performed for confirmation.

## CONCLUSIONS

This study suggests that proteins that make up the fundamental structures of the blood-CSF barrier are in their adult location already at mid-gestation in the nonhuman primate fetus and that there is little regulation of these proteins during the second half of gestation. This indicates that the basis for the blood-CSF barrier is well established in the mid-gestation fetus although functional studies are needed for confirmation. There is variable expression of genes encoding for xenobiotic metabolism. Phase I metabolism transcripts such as monoamine oxidases and epoxy hydrolases are found in significant amount, while CYPs are less abundant. In contrast, expression of genes associated with phase II metabolism appears robust and especially dependent on a rich variety of GSTs. However, there was little regulation of either phase I/II genes during development. On the other hand, some solute carriers considered being involved in drug transport showed increased expression with gestation. In particular, transcription of OATPs increased at late gestation and ought to be further examined. Transcription of antioxidants, including the inducing antioxidant systems, was high in the choroid plexus across all gestational ages suggesting that the fetal choroid plexus possess many mechanisms to deactivate reactive molecules. We have only explored the transcription of genes and further functional data is needed to better interpret the observed changes. This is particularly difficult for many of the transporters as the direction of transport is uncertain. The nonhuman primate data validates most of the previous results from rodents in relation to xenobiotic metabolisms in the choroid plexus although there are

some distinct differences on the complement of transporters and CYP enzymes that should be taken into consideration when translating data to the human.

## Supplementary Material

Refer to Web version on PubMed Central for supplementary material.

## Acknowledgments

This work was supported by NICHD 21350 (PN, CL), Swedish Research Council (VR 2012-3500, CM), Government grant in Public Health Service at the Sahlgrenska University Hospital (ALFGBG-142881, CM), European Union grant FP7 (Neurobid, HEALTHF2-2009-241778, CM & CJE), the Leducq foundation (DSRR\_P34404, CM), Åhlén Foundation (CM), Olle Enqvist Foundation (CM) and the Swedish Brain Foundation (FO2013-095, CM), Åke Wiberg Foundation (CJE), Magnus Bergvall Foundation (CJE), Wilhelm and Martina Lundgren Foundations (CJE). We would also like to thank the Bioinformatics Core Facility platform, at the Sahlgrenska Academy, University of Gothenburg.

## References

1. Ek CJ, Habgood MD, Dziegielewska KM, Saunders NR. Structural characteristics and barrier properties of the choroid plexuses in developing brain of the opossum (*Monodelphis Domestica*). *The Journal of comparative neurology*. 2003; 460:451–64. [PubMed: 12717706]
2. Liddel SA, Dziegielewska KM, Ek CJ, Habgood MD, Bauer H, Bauer HC, et al. Mechanisms that determine the internal environment of the developing brain: a transcriptomic, functional and ultrastructural approach. *PloS one*. 2013; 8:e65629. [PubMed: 23843944]
3. Strazielle N, Khuth ST, Ghersi-Egea JF. Detoxification systems, passive and specific transport for drugs at the blood-CSF barrier in normal and pathological situations. *Advanced drug delivery reviews*. 2004; 56:1717–40. [PubMed: 15381331]
4. Ghersi-Egea JF, Leininger-Muller B, Cecchelli R, Fenstermacher JD. Blood-brain interfaces: relevance to cerebral drug metabolism. *Toxicology letters*. 1995; 82–83:645–53.
5. Ek CJ, Wong A, Liddel SA, Johansson PA, Dziegielewska KM, Saunders NR. Efflux mechanisms at the developing brain barriers: ABC-transporters in the fetal and postnatal rat. *Toxicology letters*. 2010; 197:51–9. [PubMed: 20466047]
6. Gazzin S, Strazielle N, Schmitt C, Fevre-Montange M, Ostrow JD, Tiribelli C, et al. Differential expression of the multidrug resistance-related proteins ABCb1 and ABCc1 between blood-brain interfaces. *The Journal of comparative neurology*. 2008; 510:497–507. [PubMed: 18680196]
7. Ghersi-Egea JF, Strazielle N, Murat A, Jouvét A, Buenerd A, Belin MF. Brain protection at the blood-cerebrospinal fluid interface involves a glutathione-dependent metabolic barrier mechanism. *J Cereb Blood Flow Metab*. 2006; 26:1165–75. [PubMed: 16395287]
8. Collaborative Group On Drug Use In Pregnancy C. An international survey on drug utilization during pregnancy. *The International journal of risk & safety in medicine*. 1991; 2:345–9. [PubMed: 23512084]
9. Ek CJ, Dziegielewska KM, Habgood MD, Saunders NR. Barriers in the developing brain and Neurotoxicology. *Neurotoxicology*. 2012; 33:586–604. [PubMed: 22198708]
10. Kratzer I, Liddel SA, Saunders NR, Dziegielewska KM, Strazielle N, Ghersi-Egea JF. Developmental changes in the transcriptome of the rat choroid plexus in relation to neuroprotection. *Fluids and barriers of the CNS*. 2013; 10:25. [PubMed: 23915922]
11. Kroenke CD, Van Essen DC, Inder TE, Rees S, Bretthorst GL, Neil JJ. Microstructural changes of the baboon cerebral cortex during gestational development reflected in magnetic resonance imaging diffusion anisotropy. *The Journal of neuroscience: the official journal of the Society for Neuroscience*. 2007; 27:12506–15. [PubMed: 18003829]
12. Li C, McDonald TJ, Wu G, Nijland MJ, Nathanielsz PW. Intrauterine growth restriction alters term fetal baboon hypothalamic appetitive peptide balance. *The Journal of endocrinology*. 2013; 217:275–82. [PubMed: 23482706]

13. Schlabritz-Loutsevitch N, Ballesteros B, Dudley C, Jenkins S, Hubbard G, Burton GJ, et al. Moderate maternal nutrient restriction, but not glucocorticoid administration, leads to placental morphological changes in the baboon (*Papio sp.*). *Placenta*. 2007; 28:783–93. [PubMed: 17382997]
14. Ek CJ, Nathanielsz P, Li C, Mallard C. Transcriptomal Changes and Functional Annotation of the Developing Nonhuman Primate Choroid Plexus. *Frontiers in neuroscience*. 2015;9. [PubMed: 25688184]
15. Trapnell C, Pachter L, Salzberg SL. TopHat: discovering splice junctions with RNA-Seq. *Bioinformatics*. 2009; 25:1105–11. [PubMed: 19289445]
16. Trapnell C, Roberts A, Goff L, Pertea G, Kim D, Kelley DR, et al. Differential gene and transcript expression analysis of RNA-seq experiments with TopHat and Cufflinks. *Nature protocols*. 2012; 7:562–78. [PubMed: 22383036]
17. Anders S, Huber W. Differential expression analysis for sequence count data. *Genome biology*. 2010; 11:R106. [PubMed: 20979621]
18. Jancova P, Anzenbacher P, Anzenbacherova E. Phase II drug metabolizing enzymes. *Biomedical papers of the Medical Faculty of the University Palacky, Olomouc, Czechoslovakia*. 2010; 154:103–16.
19. Brown PD, Davies SL, Speake T, Millar ID. Molecular mechanisms of cerebrospinal fluid production. *Neuroscience*. 2004; 129:957–70. [PubMed: 15561411]
20. Janssen SF, Gorgels TG, Ten Brink JB, Jansonius NM, Bergen AA. Gene expression-based comparison of the human secretory neuroepithelia of the brain choroid plexus and the ocular ciliary body: potential implications for glaucoma. *Fluids and barriers of the CNS*. 2014; 11:2. [PubMed: 24472183]
21. Wolburg H, Wolburg-Buchholz K, Liebner S, Engelhardt B. Claudin-1, claudin-2 and claudin-11 are present in tight junctions of choroid plexus epithelium of the mouse. *Neuroscience letters*. 2001; 307:77–80. [PubMed: 11427304]
22. Kratzer I, Vasiljevic A, Rey C, Fevre-Montange M, Saunders N, Strazielle N, et al. Complexity and developmental changes in the expression pattern of claudins at the blood–CSF barrier. *Histochemistry and cell biology*. 2012; 138:861–79. [PubMed: 22886143]
23. Johansson PA, Dziegielewska KM, Ek CJ, Habgood MD, Liddelow SA, Potter AM, et al. Blood–CSF barrier function in the rat embryo. *The European journal of neuroscience*. 2006; 24:65–76. [PubMed: 16800861]
24. Bito LZ, Myers RE. The ontogenesis of haematoencephalic cation transport processes in the rhesus monkey. *J Physiol*. 1970; 208:153–70. [PubMed: 5499754]
25. Higgins LG, Hayes JD. Mechanisms of induction of cytosolic and microsomal glutathione transferase (GST) genes by xenobiotics and pro-inflammatory agents. *Drug metabolism reviews*. 2011; 43:92–137. [PubMed: 21495793]
26. Richard K, Hume R, Kaptein E, Stanley EL, Visser TJ, Coughtrie MW. Sulfation of thyroid hormone and dopamine during human development: ontogeny of phenol sulfotransferases and arylsulfatase in liver, lung, and brain. *The Journal of clinical endocrinology and metabolism*. 2001; 86:2734–42. [PubMed: 11397879]
27. Kiang TK, Ensom MH, Chang TK. UDP-glucuronosyltransferases and clinical drug–drug interactions. *Pharmacol Ther*. 2005; 106:97–132. [PubMed: 15781124]
28. Dallas S, Miller DS, Bendayan R. Multidrug resistance-associated proteins: expression and function in the central nervous system. *Pharmacological reviews*. 2006; 58:140–61. [PubMed: 16714484]
29. Löscher W, Potschka H. Role of drug efflux transporters in the brain for drug disposition and treatment of brain diseases. *Prog Neurobiol*. 2005; 76:22–76. [PubMed: 16011870]
30. Leslie EM, Deeley RG, Cole SP. Multidrug resistance proteins: role of P-glycoprotein, MRP1, MRP2, and BCRP (ABCG2) in tissue defense. *Toxicology and applied pharmacology*. 2005; 204:216–37. [PubMed: 15845415]
31. Wijnholds J, deLange EC, Scheffer GL, van den Berg DJ, Mol CA, van der Valk M, et al. Multidrug resistance protein 1 protects the choroid plexus epithelium and contributes to the blood–cerebrospinal fluid barrier. *J Clin Invest*. 2000; 105:279–85. [PubMed: 10675353]

32. Liddelow SA, Temple S, Mollgard K, Gehwolf R, Wagner A, Bauer H, et al. Molecular characterisation of transport mechanisms at the developing mouse blood-CSF interface: a transcriptome approach. *PloS one*. 2012; 7:e33554. [PubMed: 22457777]
33. Leggas M, Adachi M, Scheffer GL, Sun D, Wielinga P, Du G, et al. Mrp4 confers resistance to topotecan and protects the brain from chemotherapy. *Molecular and cellular biology*. 2004; 24:7612–21. [PubMed: 15314169]
34. Chavan H, Oruganti M, Krishnamurthy P. The ATP-binding cassette transporter ABCB6 is induced by arsenic and protects against arsenic cytotoxicity. *Toxicol Sci*. 2011; 120:519–28. [PubMed: 21266531]
35. Schinkel AH, Mol CA, Wagenaar E, van Deemter L, Smit JJ, Borst P. Multidrug resistance and the role of P-glycoprotein knockout mice. *Eur J Cancer*. 1995; 31A:1295–8. [PubMed: 7577039]
36. Roth M, Obaidat A, Hagenbuch B. OATPs, OATs and OCTs: the organic anion and cation transporters of the SLCO and SLC22A gene superfamilies. *British journal of pharmacology*. 2012; 165:1260–87. [PubMed: 22013971]
37. Pizzagalli F, Hagenbuch B, Stieger B, Klenk U, Folkers G, Meier PJ. Identification of a novel human organic anion transporting polypeptide as a high affinity thyroxine transporter. *Molecular endocrinology*. 2002; 16:2283–96. [PubMed: 12351693]
38. Alebouyeh M, Takeda M, Onozato ML, Tojo A, Noshiro R, Hasannejad H, et al. Expression of human organic anion transporters in the choroid plexus and their interactions with neurotransmitter metabolites. *Journal of pharmacological sciences*. 2003; 93:430–6. [PubMed: 14737013]
39. Pritchard JB, Sweet DH, Miller DS, Walden R. Mechanism of organic anion transport across the apical membrane of choroid plexus. *The Journal of biological chemistry*. 1999; 274:33382–7. [PubMed: 10559217]
40. Shu C, Shen H, Teuscher NS, Lorenzi PJ, Keep RF, Smith DE. Role of PEPT2 in peptide/mimetic trafficking at the blood-cerebrospinal fluid barrier: studies in rat choroid plexus epithelial cells in primary culture. *J Pharmacol Exp Ther*. 2002; 301:820–9. [PubMed: 12023509]
41. Ocheltree SM, Shen H, Hu Y, Keep RF, Smith DE. Role and relevance of peptide transporter 2 (PEPT2) in the kidney and choroid plexus: in vivo studies with glycylsarcosine in wild-type and PEPT2 knockout mice. *J Pharmacol Exp Ther*. 2005; 315:240–7. [PubMed: 15987832]
42. Clark J, Simon DK. Transcribe to survive: transcriptional control of antioxidant defense programs for neuroprotection in Parkinson's disease. *Antioxidants & redox signaling*. 2009; 11:509–28. [PubMed: 18717631]
43. D'Angelo B, Ek CJ, Sandberg M, Mallard C. Expression of the Nrf2-system at the blood-CSF barrier is modulated by neonatal inflammation and hypoxia-ischemia. *Journal of inherited metabolic disease*. 2013; 36:479–90. [PubMed: 23109062]
44. Oreskovic D, Klarica M. The formation of cerebrospinal fluid: nearly a hundred years of interpretations and misinterpretations. *Brain research reviews*. 2010; 64:241–62. [PubMed: 20435061]
45. Wu Q, Delpire E, Hebert SC, Strange K. Functional demonstration of Na<sup>+</sup>-K<sup>+</sup>-2Cl<sup>-</sup>-cotransporter activity in isolated, polarized choroid plexus cells. *The American journal of physiology*. 1998; 275:C1565–72. [PubMed: 9843718]
46. Speake T, Freeman LJ, Brown PD. Expression of aquaporin 1 and aquaporin 4 water channels in rat choroid plexus. *Biochimica et biophysica acta*. 2003; 1609:80–6. [PubMed: 12507761]
47. Johansson PA, Dziegielewska KM, Ek CJ, Habgood MD, Mollgard K, Potter A, et al. Aquaporin-1 in the choroid plexuses of developing mammalian brain. *Cell and tissue research*. 2005; 322:353–64. [PubMed: 16133142]



**Highlights 4620ETS**

Study of the fetal nonhuman primate choroid plexus in relation to neuroprotection

Combination of RNAseq and protein analysis

Barrier mechanisms of choroid plexus are developed in fetus

Phase I–III metabolisms and antioxidant genes are highly expressed in plexus

Fetal choroid plexus can influence xenobiotics and nutrient supply into brain

Author Manuscript

Author Manuscript

Author Manuscript

Author Manuscript

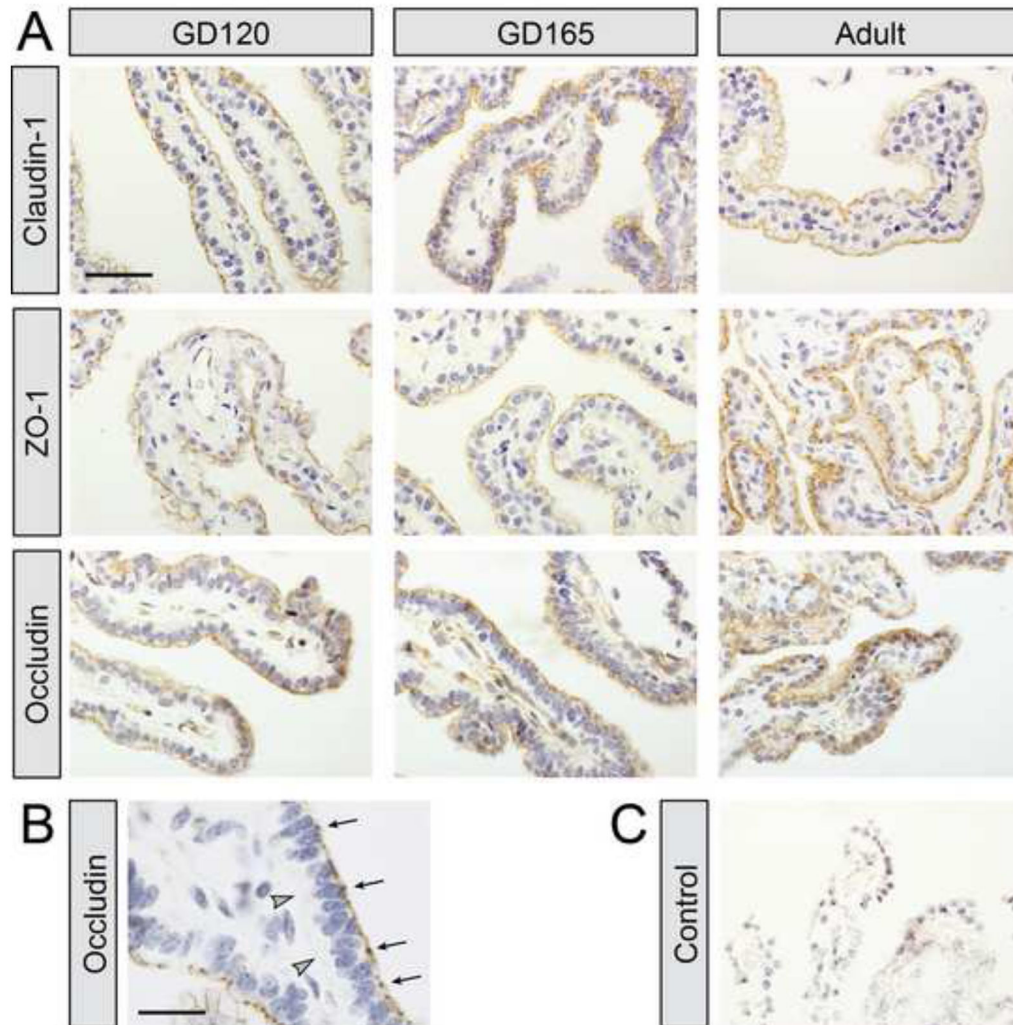


**Figure 1.**

A) Immunoreactivity for claudin-1, ZO-1 and occludin in choroid plexus of gestational day (GD) 90, GD165 fetuses and in adults. Immunoreactivity in tissue was only visible at the apical cell membrane of the epithelial cells and not in other parts of the plexus. There was no apparent difference in the staining pattern in fetuses compared to adult tissue. Tissue was counterstained with hematoxylin. B) Higher power image of occludin staining showing that staining was present on the apical side of epithelial cells (arrows), where the tight-junctions are situated, whereas no staining was present on the basal side of cells (arrowheads) in fetuses. C) Control slides where primary antibodies were omitted resulted in no staining of plexus. Scale bar is 50 $\mu$ m in A and 20 $\mu$ m in C.

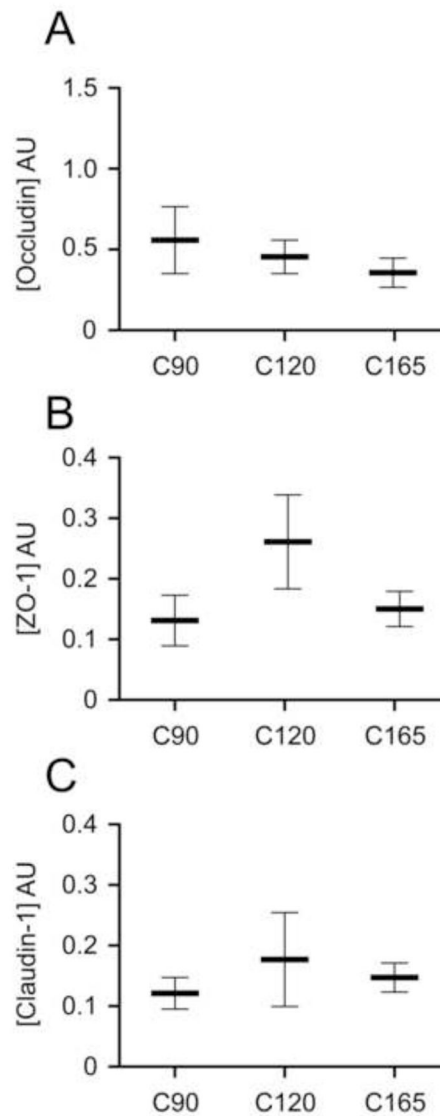


**Figure 2.** Protein quantification using western blotting of three tight-junctional associated protein occludin, ZO-1 and claudin-1 in the fetal nonhuman primate plexus at gestational day (GD) 90, 120 and 165. Western blot analysis showed only minor differences in protein levels between the three gestational ages and with no statistically significant differences (one-way ANOVA). Data are mean  $\pm$  SEM.

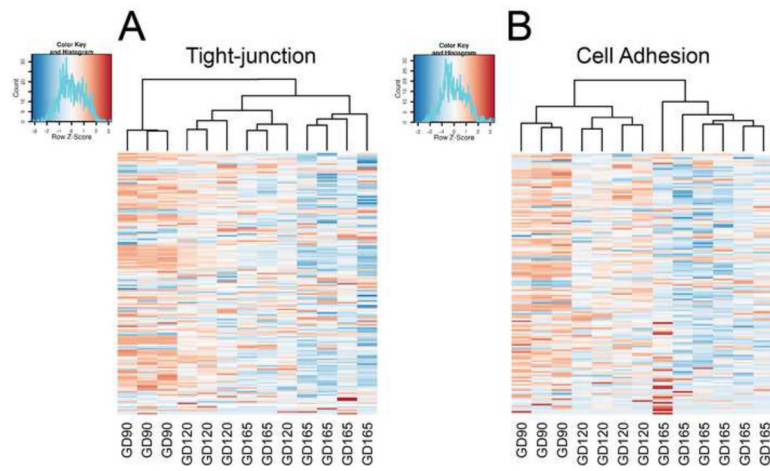


**Figure 3.** Heatmap generated from the read counts of tight-junction associated genes (A) and cell-cell adhesion genes (B) along with cluster analysis. Each column in the heatmap represents an individual animal and the cluster analysis shows which animals have the closest relationship based on these genes. Note that expression across the genes was highest at the earliest gestational age and cluster analysis shows separation of animals into their respective gestation age except the GD120 and 165 animals in A. GD - Gestational Day.

**Table 1**

Transcripts associated to Phase I Metabolism. Fold changes (FC) and adjusted *p*-values were detected between gestational day (GD) 90 and GD165.

GENE	GD90	GD120	GD165	FC	p-value
<i>CYP1B1</i>				1.49	0.857
<i>CYP2A13</i> *				2.08	0.464
<i>CYP2C8</i> *				-4.32	0.128
<i>CYP2C18</i>				-1.12	0.831
<i>CYP2C19</i>				2.21	0.235
<i>CYP2J2</i>				1.03	1.000
<i>CYP2R1</i>				1.43	0.081
<i>CYP2S1</i> *				3.02	0.026
<i>CYP2W1</i>				-25.37	0.000
<i>CYP3A5</i>				-1.23	0.849
<i>CYP4B1</i>				-1.12	0.892
<i>CYP4F12</i>				4.64	0.002
<i>CYP4V12</i>				-1.10	0.764
<i>CYP4F11</i> *				-1.25	0.812
<i>CYP4X1</i> *				1.18	0.924
<i>CYP4Z1</i> *				-4.11	0.407
<i>CYP17A1</i>				1.88	0.064
<i>CYP20A1</i>				1.25	0.314
<i>CYP21A2</i>				1.37	0.376
<i>CYP26B1</i>				-1.27	0.842
<i>CYP27A1</i>				-1.16	0.485
<i>CYP27B1</i> *				1.18	0.840
<i>CYP27C1</i>				-1.75	0.003
<i>CYP39A1</i>				1.37	0.103
<i>CYP51A1</i>				1.13	0.730
<i>MAOA</i>				-2.49	0.015
<i>MAOB</i>				1.60	0.005

Author Manuscript

Author Manuscript

Author Manuscript

Author Manuscript

GENE	GD90	GD120	GD165	FC	p-value
<i>EPHX1</i>				1.81	0.000
<i>EPHX2</i>				1.60	0.004
<i>EPHX3</i>				1.23	0.349
<i>EPHX4</i>				-2.06	0.010

\* <10 counts.

Colour indexing for number of read counts at each gestational age:

1 1000 10000 (counts)

**Table 2**

Transcripts associated to Phase II Metabolism. Fold changes (FC) and adjusted *p*-values were detected between gestational day (GD) 90 and GD165.

Gene	GD90	GD120	GD165	FC	<i>p</i> -value
<i>SULT1A1</i>				1.07	0.902
<i>SULT1A3</i>				1.13	0.679
<i>SULT1C4</i>				2.40	0.024
<i>SULT1E1</i>				-10.79	0.000
<i>SULT4A1</i>				4.37	0.490
<i>GSTA1</i> *				-2.75	0.264
<i>GSTA3</i>				-1.09	0.794
<i>GSTA4</i>				1.24	0.270
<i>GSTK1</i>				2.49	0.000
<i>GSTM1</i>				-1.29	0.266
<i>GSTM2</i>				-1.23	0.491
<i>GSTM3</i>				1.42	0.064
<i>GSTM4</i>				1.34	0.273
<i>GSTM5</i>				1.05	0.825
<i>GSTO1</i>				1.35	0.151
<i>GSTP1</i>				1.00	1.000
<i>GSTT1</i> *				-1.04	1.000
<i>GSTT2</i>				1.43	0.069
<i>GSTT4</i>				-1.03	1.000
<i>GSTZ1</i>				1.49	0.051
<i>MGST1</i>				-2.29	0.000
<i>MGST2</i>				1.94	0.003
<i>MGST3</i>				1.41	0.059
<i>LTC4S</i>				1.74	0.148
<i>PTGES</i>				-1.86	0.038
<i>GSR</i>				2.05	0.005
<i>GCLM</i>				1.04	0.908
<i>GCLC</i>				1.26	0.275

Author Manuscript

Author Manuscript

Author Manuscript

Author Manuscript

Gene	GD90	GD120	GD165	FC	p-value
<i>GSS</i>	Red	Red	Red	-1.02	0.959
<i>UGT3A1</i> *	Light Red	Light Red	Light Red	-3.05	0.729
<i>NAT1</i>	Light Red	Light Red	Light Red	-1.96	0.169
<i>NAT2</i> *	Light Red	Light Red	Light Red	1.06	1.000
<i>TPMT</i>	Red	Red	Red	1.42	0.090
<i>COMT</i>	Dark Red	Dark Red	Dark Red	1.24	0.377

\* <10 counts.

Colour indexing for number of read counts:





**Table 3**

Transcripts for ATP-binding cassette proteins. Fold changes (FC) and adjusted *p*-values were detected between gestational day (GD) 90 and GD165.

Gene ID	GD90	GD120	GD165	FC	<i>p</i> -value
<i>ABCB1</i>				-2.22	0.007
<i>ABCB6</i>				1.01	0.998
<i>ABCB7*</i>				-1.41	0.549
<i>ABCB8</i>				1.81	0.112
<i>ABCB9</i>				-1.13	0.776
<i>ABCB10</i>				1.10	0.751
<i>ABCC1</i>				-2.37	0.000
<i>ABCC2</i>				-1.38	0.076
<i>ABCC3*</i>				-1.53	0.561
<i>ABCC4</i>				2.44	0.000
<i>ABCC5*</i>				-1.59	0.401
<i>ABCC7</i>				-1.99	0.142
<i>ABCC8*</i>				1.07	0.977
<i>ABCC9</i>				-1.49	0.259
<i>ABCC10</i>				-1.53	0.024
<i>ABCG2</i>				-1.91	0.091

\* <10 counts.

Colour indexing for number of read counts:



**Table 4** Transcripts for solute carriers in SLCO, SLC15/22/47 families. Fold changes (FC) and adjusted *p*-values were detected between gestational day (GD) 90 and GD 165.

Gene	GD90	GD120	GD165	FC	<i>p</i> -value
<i>SLCO1A2</i>	Red	Red	Red	5.72	0.000
<i>SLCO1B1</i>	Light Red	Light Red	Light Red	3.27	0.018
<i>SLCO1B3</i>	Red	Dark Red	Dark Red	1.90	0.000
<i>SLCO1C1</i>	Light Red	Light Red	Light Red	27.5	0.000
<i>SLCO2A1</i>	Light Red	Light Red	Light Red	2.52	0.011
<i>SLCO2B1</i>	Light Red	Light Red	Light Red	1.64	0.046
<i>SLCO3A1</i>	Red	Red	Red	1.49	0.025
<i>SLCO4A1*</i>	Light Red	Light Red	Light Red	-5.97	0.094
<i>SLC15A2</i>	Light Red	Light Red	Light Red	-2.34	0.031
<i>SLC15A3</i>	Light Red	Light Red	Light Red	-1.17	0.518
<i>SLC15A4</i>	Red	Red	Red	-1.07	0.795
<i>SLC22A2</i>	Light Red	Light Red	Light Red	6.53	0.626
<i>SLC22A3*</i>	Light Red	Light Red	Light Red	-1.20	0.982
<i>SLC22A5</i>	Red	Red	Red	-1.09	0.779
<i>SLC22A6</i>	Light Red	Light Red	Light Red	1.15	0.620
<i>SLC22A8</i>	Dark Red	Dark Red	Dark Red	2.31	0.003
<i>SLC22A15</i>	Light Red	Light Red	Light Red	-1.09	0.887
<i>SLC22A16*</i>	Light Red	Light Red	Light Red	-2.40	0.443
<i>SLC22A18</i>	Light Red	Light Red	Light Red	1.26	0.522
<i>SLC22A20</i>	Red	Red	Red	1.24	0.774
<i>SLC22A23</i>	Light Red	Light Red	Light Red	-1.31	0.242
<i>SLC47A1</i>	Light Red	Light Red	Light Red	4.47	0.000
<i>SLC47A2</i>	Light Red	Light Red	Light Red	7.62	0.000

\* <10 counts.

Colour indexing for number of read counts:

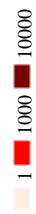


**Table 5**

Transcripts for antioxidant associated genes. Fold changes (FC) and adjusted *p*-values were detected between gestational day (GD) 90 and GD165.

Gene	GD90	GD120	GD165	FC	<i>p</i> -value
<i>SOD1</i>	Dark Red	Dark Red	Dark Red	2.39	0.000
<i>SOD2</i>	Light Red	Light Red	Light Red	1.39	0.138
<i>SOD3</i>	Light Red	Light Red	Light Red	21.9	0.000
<i>CCS</i>	Light Red	Light Red	Light Red	1.34	0.184
<i>PGC1A</i>	Light Red	Light Red	Light Red	1.75	0.002
<i>PGC1B</i> *	Light Red	Light Red	Light Red	-1.98	0.565
<i>NRF1</i>	Dark Red	Dark Red	Dark Red	-1.18	0.420
<i>NRF2</i>	Light Red	Light Red	Light Red	1.35	0.135
<i>KEAP1</i>	Light Red	Light Red	Light Red	-1.01	0.986
<i>HMOX1</i>	Light Red	Light Red	Light Red	1.45	0.714
<i>HMOX2</i>	Light Red	Light Red	Light Red	1.28	0.221

\* <10 counts.

Colour indexing for number of read counts:



**Table 6** Transcripts for genes associated with CSF production. Fold changes (FC) and adjusted *p*-values were detected between gestational day (GD) 90 and GD165.

Gene	GD90	GD120	GD165	FC	<i>p</i> -value
<i>AQP1</i>	Dark Purple	Dark Purple	Dark Purple	1.92	0.000
<i>AQP3</i>	Light Orange	Light Orange	Light Orange	1.01	0.980
<i>AQP5*</i>	Light Orange	Light Orange	Light Orange	-1.01	1.000
<i>AQP7*</i>	Light Orange	Light Orange	Light Orange	2.40	0.200
<i>AQP8*</i>	Light Orange	Light Orange	Light Orange	1.46	0.561
<i>AT1A2</i>	Dark Red	Dark Red	Dark Red	3.63	0.019
<i>AT1A3</i>	Light Orange	Light Orange	Light Orange	-1.07	1.000
<i>AT1B1</i>	Dark Red	Dark Red	Dark Red	4.11	0.000
<i>AT1B2</i>	Dark Red	Dark Red	Dark Red	1.83	0.000
<i>AT1B3</i>	Dark Red	Dark Red	Dark Red	-1.27	0.222
<i>CA1</i>	Light Orange	Light Orange	Light Orange	8.39	0.425
<i>CA2</i>	Dark Red	Dark Red	Dark Red	1.11	0.734
<i>CA4</i>	Light Orange	Light Orange	Light Orange	1.14	0.824
<i>CA9</i>	Light Orange	Light Orange	Light Orange	-1.94	0.035
<i>CA12</i>	Dark Purple	Dark Purple	Dark Purple	1.06	0.960
<i>CA13</i>	Light Orange	Light Orange	Light Orange	2.61	0.007
<i>CA14</i>	Dark Red	Dark Red	Dark Red	1.08	0.867
<i>SLC4A4</i>	Light Orange	Light Orange	Light Orange	2.18	0.451
<i>SLC4A5</i>	Dark Red	Dark Red	Dark Red	-1.17	0.431
<i>SLC4A7*</i>	Light Orange	Light Orange	Light Orange	-2.28	0.260
<i>SLC4A8</i>	Light Orange	Light Orange	Light Orange	2.57	0.000
<i>SLC12A2</i>	Dark Red	Dark Red	Dark Red	1.40	0.049
<i>SLC12A5</i>	Light Orange	Light Orange	Light Orange	3.18	0.418
<i>SLC12A7</i>	Dark Red	Dark Red	Dark Red	-1.20	0.356
<i>CLCN3</i>	Light Orange	Light Orange	Light Orange	-2.74	0.000
<i>CLCN5*</i>	Light Orange	Light Orange	Light Orange	1.18	0.992
<i>CLCN7</i>	Dark Red	Dark Red	Dark Red	1.00	1.000

Author Manuscript

Author Manuscript

Author Manuscript

Author Manuscript

Gene	GD90	GD120	GD165	FC	p-value
<i>KCNA4</i>				-4.65	0.005
<i>KCNA5</i>				1.37	0.633
<i>KCNE1</i>				-1.32	0.470
<i>KCNFI</i>				-1.23	0.428
<i>KCNK1</i>				-1.68	0.675
<i>KCNH2</i>				1.94	0.000
<i>KCNK1</i>				2.63	0.022
<i>SCN1B</i>				1.59	0.093
<i>SCN2A</i> *				1.91	0.912
<i>SCN2B</i>				-1.60	0.507
<i>SCN4A</i> *				30 -2.19	0.470
<i>SCN4B</i>				-3.10	0.278
<i>SCN5A</i>				-4.88	0.000
<i>SCN8A</i>				1.18	0.618

\* <10 counts.

Colour indexing for number of read counts:

